ADVANCED HIGH TEMPERATURE INSTRUMENTATION FOR HOT SECTION RESEARCH APPLICATIONS

D. R. Englund and R. G. Seasholtz
National Aeronautics and Space Administration
Lewis Research Center
Cleveland, Ohio

ABSTRACT

Programs to develop research instrumentation for use in turbine engine hot sections are described. These programs were initiated to provide improved measurements capability as support for a multidisciplinary effort to establish technology leading to improved hot section durability. Specific measurement systems described here include heat flux sensors, a dynamic gas temperature measuring systems, laser anemometry for hot section applications, an optical system for viewing the interior of a combustor during operation, thin film sensors for surface temperature and strain measurements, and high temperature strain measuring systems. The paper will describe the state of development of these sensors and measuring systems and, in some cases, will show examples of measurements made with this instrumentation. The paper covers work done at the NASA Lewis Research Center and at various contract and grant facilities.

INTRODUCTION

The Turbine Engine Hot Section Technology (HOST) Program was started by NASA in the late 1970's in order to develop technology leading to improved hot section durability. The program was a multidisciplinary effort involving structures, surface protection, fatigue, combustion, heat transfer, and instrumentation. The objective of the instrumentation portion of the program was to develop improved measurements capability to measure the environment within the hot section and measure the response of hot section components to that imposed environment. Instrument development programs that resulted included the following:

(1) Development of sensors for measuring the heat flux on combustor liners and turbine airfoils.

(2) Development of a system to measure the fluctuating component of combustor exit temperature with a frequency response to 1000 Hz.

(3) Development of laser anemometer techniques for applications in hot sections.

(4) Development of an optical system for viewing the interior of a combustor during operation.

(5) Development of high temperature strain measuring systems.

In addition to this, a major effort was started just prior to the start of HOST to develop thin film sensors for applications in hot sections, particularly for the measurement of turbine airfoil surface temperature.

This paper will describe the state of development of these sensors and measuring systems and, in some cases, will show examples of measurements made with this new instrumentation. The work described was done at the NASA Lewis Research Center and at various contract and grant facilities.

HEAT FLUX SENSORS

One of the important environmental parameters in the hot section is heat flux. The heat flux is one of the variables in the heat balance equation which establishes the cooling requirements and the anticipated surface temperature of a hot section component. There is not sufficient knowledge of heat transfer coefficients under engine operating condition to permit prediction of surface temperatures to within acceptable accuracy. This is especially true as heat fluxes approach 1 MW/m^2. Initial work was directed at developing sensors for use in combustor liners (Atkinson et al., 1983; Atkinson and Strange, 1982; Atkinson et al., 1985a). In later work sensors were mounted into air cooled blades and vanes (Atkinson et al., 1984; Atkinson et al., 1985b).

Sensor designs followed conventional concepts in which the temperature difference proportional to heat conduction through the sensor body is measured. Differential thermocouples using the sensor body material as part of the circuit were used to measure the temperature differences. Calibrations (Holanda, 1984) were made of the thermoelectric potential of a number of engineering alloys and these established the validity of this approach, which considerably simplified fabrication.

Figures 1 and 2 show the sensors that were developed for combustor liners. The sensor is built into a Hastelloy X disk 0.8 cm in diameter and the same thickness as the liner. After calibration of the sensor

the disk is welded into a hole cut in the liner. Figure 1 shows the embedded thermocouple sensor. The disk is grooved so that 0.25 mm outside diameter sheathed, single conductor thermocouple wire can be laid into the grooves and covered with weld material. The thermocouple wires are ISA Type K, Chromel-Alumel, and single conductor leads are used so as to maintain good insulation resistance between the wire and the external metal sheath. Grounded Alumel junctions are located on the hot and cold side of the sensor body and a Chromel junction is added to the cold side. A voltage measurement between the Alumel leadwires (i.e., using the Alumel-Hastelloy X-Alumel differential thermocouple) provides the hot-to-cold side temperature difference proportional to the one-dimensional heat flow through the sensor body at that point. A measurement using the conventional Chromel-Alumel thermocouple provides the cold side temperature of the sensor.

Figure 2 shows a Gardon Gage sensor. In this case the sensor body has a 1.5 mm diameter cylindrical cavity on the cold side so that a thin membrane of material is left on the hot side. Alumel wires are positioned so the junctions are formed with the Hastelloy X at the center of the membrane and halfway up the sidewall of the cavity. A Chromel wire junction is also made on the sidewall of the cavity. After the thermocouples are installed, the cavity is filled with ceramic cement.

Sensors of the embedded thermocouple and Gardon Gage types have also been built into air cooled blades and vanes. In the case of turbine blades, two-piece blades were used and the sensors were installed from the cooling passage side of the blade. The two blade halves were then joined by brazing. In the case of vanes, sections of the vane wall opposite to the desired sensor sites were removed and the sensors were installed through these "windows." Figure 3 depicts the installation process on a turbine vane.

The heat flux sensors were calibrated over a heat flux range up to 1.7 MW/m^2 and a temperature range to 1250 K. The calibrations were accomplished by imposing a known radiant heat flux on the hot side surface of the sensor and flowing cooling air over the cold side surface. The hot side surface was coated with a high temperature black paint with a measured absorptance and emittance of 0.89 over the test temperature range. In all cases the reference temperature was measured and used to estimate the hot side surface temperature so that energy being radiated away from the hot surface could be calculated and taken into account. Estimates of the convective heat flow from the hot surface were also made and used in the heat balance.

The heat flux sensor calibration systems used banks of tungsten filament lamps enclosed in quartz tubes as heat flux sources; the most powerful of these systems provided heat fluxes up to 1.7 MW/m^2. The quartz lamp rigs were capable of long time and cyclic operation at reduced heat fluxes. Thermal cycling and drift tests were run on these sensors using this capability.

Calibration and performance tests on heat flux sensors have indicated that measurements can be achieved fairly readily on combustor liners, but that accurate measurements on airfoils are difficult to achieve. Combustor liner measurements have been made both at a contractor facility and at NASA Lewis using sensors whose calibration uncertainty is within ± 5 percent of a nominal full scale heat flux of 1 MW/m^2. Figure 4 shows an instrumented combustor liner segment. Figure 5 compares measured values of heat flux conducted through a combustor liner and radiant flux incident on the liner at different combustor pressure levels. The radiant heat flux was measured with a commercial radiometer. The combustor liner in this test was the type with louver lips and bleed holes to provide film cooling of the hot side surface. The data of Fig. 5 indicate that there is significant convective cooling of the hot side surface of the combustor.

Test results from sensors mounted in turbine airfoils indicate that these sensors are sufficiently sensitive to transverse gradients in heat flux and temperature that applications in blades and vanes must be carefully evaluated. The greater complexity of the airfoils (e.g., high surface curvature and cooling passage structure) causes more severe gradients than were encountered in combustor liners. Sensitivity to transverse gradients is especially apparent in the Gardon gage sensor because of its lack of symmetry.

DYNAMIC GAS TEMPERATURE MEASURING SYSTEM

Another important environmental parameter in the hot section of a turbine engine is the gas temperature. In general, most attention has been directed at the time-average value of gas temperature rather than the fluctuating component of gas temperature. It is generally agreed that there may be significant temperature fluctuation in the gas exiting a combustor due to incomplete mixing of the combustion and dilution gas streams. It is also agreed that thermal cycling of the surfaces of turbine airfoils can result in spalling of oxide films used for corrosion projection and thus shorten the life of the airfoils. Development of a system to measure gas temperature fluctuations was undertaken to aid in modeling combustor flow and in studying the thermal cycling of airfoil surfaces. Combustor modeling requirements set the frequency response goal at 1000 Hz.

The approach used in this work was to devise a way to determine in situ the compensation spectrum required to correct for the limited frequency response of a thermocouple probe located in the gas stream. Frequency compensation has often been used, especially with hot wire anemometers, in the measurement of dynamic flow phenomena. The problem with this technique when applied to a thermal element in a flow stream is that the required compensation spectrum is a function of both the thermal mass of the thermocouple and the coefficient for heat transfer between the gas and the thermocouple. This heat transfer coefficient is a function of the gas flow conditions. Each time the flow conditions change, the compensation spectrum must be redetermined. In some cases estimates of the compensation spectrum may be sufficient; in this case it was important to be able to make in situ determinations of the compensation spectrum.

The system that was developed (Elmore et al., 1984; Elmore et al., 1983; Elmore et al., 1986a and b; Stocks and Elmore, 1986) uses a dual element thermocouple probe such as shown in Fig. 6. Thermocouples are formed with carefully butt welded junctions so that there is no variation in diameter in the region of the junction. These thermocouples are each supported across a pair of support posts so that they are parallel cylinders in cross flow and are in close enough proximity (approx 1 mm) so that they are measuring the same temperature. The thermocouple wires and the support posts are made from Pt-30Rh/Pt-6Rh. The thermocouple junctions are midway between the support posts. The two thermocouples have different diameters, commonly 75 and 250 μm. Neither of these thermocouples have the desired frequency response, but a comparison of their dynamic signals can lead to the needed compensation spectrum. The technique is based on the use of the ratio of the Fourier coefficients of the dynamic signals for frequencies in the range where the signals

become attenuated. In the system which has been developed, the signals are recorded on magnetic tape and processed in a general purpose digital computer at a later time. The data reduction process takes approximately 5 min for each flow condition for which a new compensation spectrum must be calculated.

Elmore et al. (1986 a and b) describe experiments to demonstrate the frequency response of the system. Measurements were made in a specially designed test rig and in the exhaust of an atmospheric burner. Comparisons were made between the dynamic gas temperature system and very fine wire resistance thermometers (6 and 12 μm wire diameters). At low frequencies (below 250 Hz) with reasonable temperature fluctuations agreements within ±23 percent were obtained. Poorer results were obtained at higher frequencies but here the temperature fluctuations were so small as to make the data questionable.

This system has been used to measure fluctuating temperature in both turbine engines and in combustor test rigs. A sample of data from a turbine engine test is shown in Fig. 7. In this test the probe was located between first-stage turbine vanes. For the data shown in Fig. 7, the engine was operating at an intermediate power level and the average gas temperature was 1200 K. Figure 7 shows four plots of fluctuating temperature versus time. Figures 7(a) and (b) shown the uncompensated signals from the 75 and 250 μm thermocouples. Note that the temperature scales on these plots have been adjusted so as to show the waveforms. Also note that the rms temperature fluctuation is listed on each plot. Figure 7(c) shows the compensated temperature fluctuation from the 75 μm thermocouple, and Fig. 7(d) show an expanded time segment of the compensated signal. The rms value of the compensated temperature fluctuation is 218 K and the peak-to-peak fluctuation is approximately ±500 K.

LASER ANEMOMETRY

The laser anemometer (LA) has become a valuable tool in turbine engine research, providing data that would be almost impossible to gather using conventional instrumentation. However, the use of LA in turbomachinery has proven to be one of its more difficult applications. Turbomachinery components are typified by small passages and highly accelerated, high-velocity flows. This leads to the need for small seed particles that will faithfully follow the flow. Unfortunately, small particles are weak light scatterers, which result in low signal levels. In addition, measurements in small passages require great care in the design of the optics to minimize the amount of detected surface-scattered laser light (flare). All these considerations must be included in the design of an LA to obtain the maximum amount of accurate data in minimum experimental run times.

HOST experiments where researchers planned to use LA were studied to determine critical technology areas. Research programs were then conducted in several of these areas including optical design, seed generation, signal processing, and data acquisition. An ambient pressure, laboratory-type combustor was used to evaluate optical systems and signal processors.

Modeling of Fringe-Type LA

The fringe-type LA was analyzed (Seasholtz et al., 1984) using the Cramer-Rao lower bound for the variance of the estimate of the Doppler frequency as a figure of merit. Mie scattering theory was used to calculate the Doppler signal with both the amplitude and phase of the scattered light taken into account. The noise due to wall scatter (flare) was calculated using the wall bi-directional reflectance distribution function (BRDF) and the irradiance of the incident beams. A procedure was developed to find the optimum aperture stop shape for the probe volume located a given distance from a wall. Figure 8 shows SNR as a function of probe volume to wall distance for two optical systems with optimum aperture masks.

The BRDF was measured for a number of uncoated materials, finishes, and surface coating. Data were obtained for "as machined" surfaces, polished surfaces, glossy black coatings, and flat back coatings. Based on these data, the best surface for LA applications appears to be a glossy black coating. Although a black glossy surface has a relatively large specular reflection, the diffusely reflected light, which is usually of greatest concern in LA systems, is substantially less than the diffusely reflected light from a flat black coating.

Seeding

Particle characteristics necessary for hot section LA are primarily the same as low temperature LA, with the exception that the particles must retain those characteristics at high temperatures. Based on a survey of available materials, a particular grade of aluminum oxide (nominal 1 μm diam) was selected. A commercial, high-volume fluidized bed was chosen to disperse the seed particles.

An experiment was also conducted to determine the feasibility of using chemically formed seed for hot flows. Titanium tetrachloride vapor was injected into the flow where it reacted with the water vapor to form titanium dioxide and hydrochloric acid (HCl). The titanium dioxide is a suitable high temperature seed material; it has a sub-micron size, and it is produced in large quantities. However, the HCl, if not neutralized, can cause corrosion, which limits the application of this seeding technique.

Preprocessor for Fringe-Type LA

The quality of data from an LA is critically dependent on a number of control settings of the signal processor. These typically include the optical detection system gain (determined by the photomultiplier tube high voltage and amplifier gain) and the electrical filters used to remove the low frequency pedestal component and to reduce shot noise. A study was made to quantify the effect of filters on measurement accuracy (Oberle and Seasholtz, 1985). Several common filter designs were examined. It was shown that both the filter type and the cutoff frequencies must be carefully selected to avoid filter-induced errors in counter-type processors. It was shown that these errors are particularly significant for probe volumes containing a small number of fringes and for highly turbulent flow.

Experiments in turbomachinery test facilities usually have high operational costs, so it is necessary to acquire the desired data in a minimum time. Extensive operator interaction with the instrumentation during a test run is usually not desirable. To provide for efficient data acquisition and correct processor settings, a computer-controlled interface (called a preprocessor) was designed, fabricated, and tested (Oberle, 1987). The preprocessor (Fig. 9) amplifies the signal from the photodetector, filters it using both low- and high-pass filters, and then routes it to the counter processor.

The chief virtue of the preprocessor is that it provides direct computer control of the PMT high voltage, the rf gain (50 dB of amplification and a programmable attenuator are used to provide control over the range -77 dB to +50 dB in 1 dB steps), and selection

of the low- and high-pass filters (8 low-pass and 8 high-pass). In addition, the preprocessor provides computer control of the seed generator and allows computer monitoring of the PMT dc current. With proper software, the preprocessor will allow the researcher to preprogram the various processor settings based on the expected flow conditions. It will also be possible to use "smart" adaptive software to select the proper settings based current measurement parameters such as the frequency, turbulence intensity, and noise level.

Four-Spot LA

The conventional fringe-type LA has a large acceptance angle (i.e., it can measure velocities having a wide range of flow angles), but it has a relatively large probe volume. This large probe volume limits the closest measurements to about 1 mm from surfaces. The conventional time-of-flight LA (aka two-spot or transit LA) has a much smaller probe volume, which allows it to measure much closer to surfaces. However, the two-spot LA has a very limited acceptance angle, which greatly reduces its capabilities in highly turbulent flows.

The need for an anemometer incorporating the large acceptance angle of the fringe LA and the ability of the two-spot LA to measure close to walls led to the development of a new type of time-of-flight LA (Lading, 1983; Wernet and Edwards, 1986). The new Four-Spot LA, shown in Fig. 10, incorporates two features. One is the use of elliptical rather than circular spots to give a large acceptance angle. (This use of two elliptical spots is also called a two-dash or two-sheet time-of-flight LA.) The other feature, which is unique, is the use of four beams arranged to form two pairs of orthogonally polarized, partially overlapping spots. This allows the use of an optical method to accurately determine the start and stop timing signals. Previously, delay-and-subtract techniques were used to generate the timing signals. The optical method, unlike delay and subtract, is independent of the velocity. This is advantageous in highly turbulent flow or in other flows with a wide range of velocities.

The Four-Spot LA was designed, fabricated, and successfully tested. Measurements were obtained as close as 75 μm from a normal surface (Wernet, 1987). Comparison measurements were also made using the four-spot LA, a two-spot LA, and a fringe-type LA in the vicinity of a single turbine vane mounted in the exhaust of the open jet burner (Wernet and Oberle, 1987).

Windows and Correction Optics

In turbomachinery studies it is highly desirable to obtain measurements without altering the flow being studied. With optical techniques this means that the window contour should match the internal flow passage contour. One Lewis HOST facility was a 508 mm diameter, single stage, axial flow turbine facility. Two cylindrical windows were designed to allow measurements within the stator and rotor passages. These windows, however, act as cylindrical lenses that introduce aberrations into the LA optical system. If not corrected, these aberrations can greatly degrade the measurements or even prevent any measurements. A monochromatic correction optic (Fig. 11) was designed for this application (Wernet and Seasholtz, 1987). The addition of the correction optic restores the diffraction limited performance of the optical system.

COMBUSTOR VIEWING SYSTEM

Another way to determine the response of a component to the hot section environment is to monitor visual images of the component during operation. This is not likely to produce quantitative data but, in some cases, qualitative data are sufficient or even preferable. A case in point is the Combustor Viewing System (Morey, 1984; Morey, 1985). This system was designed to provide recorded images of the interior of a combustor during operation; the objective was to produce a visual record of some of the causes of premature hot section failure.

The Combustor Viewing System consists of a water cooled optical probe, a probe actuator, an optical interface unit that couples the probe to cameras and to an illumination source, and system controls. The probe with its actuator is designed to mount directly on an engine or a combustor. The probe is 12.7 mm in diameter, small enough to fit into an igniter port. The actuator provides a rotational motion of ±180° and radial insertion to a maximum depth of 7.6 cm. Two probes were built to use with the system. The wide field-of-view probe can be fitted with lenses for 90° and 60° fields-of-view, with the viewing axis oriented 45° to the axis of the probe. The narrow field-of-view probe has lenses for 35° and 13° fields-of-view that are oriented 60° relative to the probe axis. Both probes are water cooled and gas purged and are capable of operating within the primary combustion zone of a combustor.

Figures 12(a) and (b) show cross section views of the two probes. In each case an image conduit is used to transfer the image through the length of the probe. The image conduit is a fused bundle of fibers 3 mm in diameter and consists of about 75 000 fibers 10 μm in diameter. Each of these fibers corresponds to a picture element. The image conduit is 33 cm long and is coupled to a flexible fiber bundle which connects the probe to the optical interface unit. Each probe is also equipped with two 1 mm diameter plastic clad fused quartz fibers used for illumination when required.

The optical interface unit contains cameras, filters, and an illumination source. Either film or video cameras can be remotely selected and up to eight filters can be inserted into the viewing path. The illumination source is a mercury arc lamp which is focused on the ends of the illumination fibers.

This system has been used in both combustor and full scale engine tests. Although the original use for the system was in combustor liner durability studies, the system also has capability as a flowpath diagnostic device. It has been used to examine light off and blowout characteristics and appears to have considerable potential for other time dependent phenomena and for flame radiometry. Subsequent to the initial development program, additional systems were built and put into service in aircraft engine development work and in testing turbine engines used to generate electrical power.

HIGH TEMPERATURE STRAIN MEASURING SYSTEMS

The most ambitious instrumentation development effort in this program is the development of high-temperature strain measuring systems. The target goal for this work is to measure strain (approx 2000 microstrain, maximum) at temperatures up to 1250 K with an uncertainty of ±10 percent. This requirement is for relatively short term testing; a 50 hr sensor life is considered sufficient. Spatial resolution of the order of 3 mm is desired and where measurements are required on blades or vanes, large temperature gradients are anticipated. In general, the requirement is for steady-state measurements as differentiated from dynamic (fluctuating component only) measurements.

The principal candidate for making such measurements under similar but lower temperature conditions (less than approx 700 K) is the resistance strain gage. However, at the higher temperatures, strain measurements become increasingly difficult and the commonly used strain gages are marginal at best. As the required temperature range increases, the magnitude of the correction for apparent strain becomes substantially larger than the strain signal and the uncertainty of the correction is excessive. To meet the goals listed above, the uncertainty of the apparent strain correction must be less than ±200 microstrain. This requirement translates to a repeatability of the resistance versus temperature for the mounted strain gage to be well within ±400 parts per million (ppm), based on a gage factor of two.

We made an extensive study of potentially useful high-temperature static strain measurement techniques (Hulse et al., 1987a). As a result of this study, we are pursuing the following to improve our high temperature strain measuring capability:

(1) developing improved high temperature strain gages
(2) learning how better to use available strain gages
(3) developing optical strain measuring systems as alternatives to strain gages

The following section will discuss these three areas of work.

Development of Improved High Temperature Strain Gages

In attempting to develop improved high temperature strain gages, we are emphasizing development of alloys with very repeatable resistance versus temperature characteristics (Hulse et al., 1985; Hulse et al., 1987b). We tested a number of alloy compositions from five alloy families. These alloy families are FeCrAl, NiCrSi (Nicrosil), PtPdMo, PdCr, and PtW. In all cases except for the thermocouple alloy Nicrosil, we looked at a range of compositions. Alloy sample were cast into rods and then machined into suitable test samples. Measurements were made of resistance versus temperature over a number of cycles in which cooling rates were varied from 50 to 250 K/minute. Additional tests included oxidation (weight gain method) and resistance drift for up to 3 hr in air at 1250 K. The results of these tests indicated that two alloys, one in the FeCrAl family and one in the PdCr family, had the best potential for high temperature strain gage applications.

The FeCrAl alloy was designated as "Mod 3." The fractional resistance change with temperature for this alloy at temperatures up to 1250 K is compared with the commercial Kanthal A-1 (also FeCrAl) alloy in Fig. 13. In this case both alloys were annealed for 2 hr at 1150 K prior to testing. The resistance change of the Mod 3 alloy is much less than that of the Kanthal A-1 alloy and shows comparatively little change for different cooling rates. This alloy does, however, exhibit different resistance versus temperature characteristics, depending on previous thermal history. Figure 14 illustrates this effect for exposure to 1250 K air for times ranging from 10 to 105 hr. Because of this effect, work on this alloy has been de-emphasized in favor of the PdCr alloy.

The PdCr alloy has a resistance versus temperature curve which is characteristic of a solid solution alloy with no phase or internal structure changes being evident. The resistance is essentially linear with temperature and not affected by changes in cooling rate or previous thermal history. Cycle-to-cycle repeatability of the fractional change in resistance with temperature is excellent. Tests over four thermal cycles showed an average (over the temperature range) standard deviation of 130 ppm. The greatest variation was at approximately 700 K with a standard deviation of 245 ppm. The long term drift of cast samples of this alloy at 1100 and 1250 K in air and in argon is shown in Fig. 15. It should be noted that these data imply a repeatability in resistance measurement to the order of 100 ppm; it is likely that some of the fluctuation in these curves is attributable to the measuring system rather than the resistance of the alloy samples.

The repeatability of the PdCr alloy is the property that we feel is essential for high-temperature strain gage work. However, there are other properties required for good strain gages and the PdCr alloy may not be ideal considering these properties. The temperature coefficient of resistance is high enough that temperature compensation will be required; the added complication and the larger gage size required for this will have to be accommodated. Other potential problems such as oxidation resistance of high surface-to-volume ratio thin films and fine wires, gage factor changes with temperature, and the elastic/plastic strain properties are still under investigation.

Work With Available Strain Gages

Learning how best to use available strain gages in high-temperature applications requires that considerable experimental work be done to explore strain gage characteristics and devise optimum procedures for specific applications. Such work is very time consuming, especially when tests at many different temperatures are required. Consequently, one of our objectives in this work was to establish a computer controlled testing capability at NASA Lewis so that testing could be accomplished with minimal operator attention.

The automated strain gage test laboratory has the capability to measure apparent strain and gage factor over a range of temperatures from 300 to 1370 K. The laboratory has two ovens (one of which contains a test fixture for a constant strain beam), a computer controlled actuator for deflecting the beam, strain gage and temperature instrumentation, and a personal computer for controlling the tests and collecting the data. Communication between various parts of the system is accomplished using both an IEEE-488 data bus and an RS-232 serial interface. A very versatile control program was developed that allows us to construct a variety of test profiles by entering a series of temperatures and command statements into a data set. Figure 16 shows a block diagram of the system.

One approach to better utilization of available strain gages is outlined by Stetson (1984). In this work using Kanthal A-1 alloy, it was determined that the apparent strain of the gage was strongly affected by the rate at which the gage was cooled from the highest use temperature. Further, the apparent strain for the next thermal cycle followed that established by the cooling part of the previous cycle; a repeatable apparent strain could be obtained if the cooling rate could be reproduced during each thermal cycle. This implies that an accurate apparent strain correction could be obtained by matching the cooling rate during calibration to that which would be impressed on the strain gage during use. It is necessary, of course, that the cooling rates be controllable during use and that is not always possible. But for the work of Stetson (1984), the cooling rates could be matched and, although it took considerable effort, the result was usable static strain measurements at temperatures up to 950 K.

Work based on controlled cooling rates has also been undertaken at NASA Lewis. Hastelloy X plates 13

by 20 cm were instrumented with Kanthal A-1 and Chinese FeCRAl 700 °C (Wu et al., 1981) strain gages. A plate holding fixture was made that permitted cooling gas to flow over the plate uniformly so as to get controlled cooling rates. The Kanthal A-1 gages were mounted using a flame sprayed alumina and ceramic cement process and the Chinese gages were mounted with a Chinese ceramic cement using directions supplied with the gages. The plates were also instrumented with 10 thermocouples so as to measure the temperature distribution at the strain gages. Apparent strain measurements were made over a temperature range from 300 to 950 K with cooling rates controlled at 0.1, 1.0, and 5.6 K/sec. Figure 17 shows the resulting resistance versus temperature data. Plotted here are fractional changes in resistance for one each of the Kanthal A-1 and Chinese gages for the three different cooling rates. The data show the Kanthal gage to be strongly dependent on cooling rate but repeatable in resistance at the maximum temperature. The resistance of the Chinese gage is independent of cooling rate at both 300 and 950 K, but at intermediate temperatures the curves deviate depending on cooling rate. The maximum deviations in these curves occur in the temperature range from 650 to 800 K, roughly the same region for which high drift rates have been reported for the Chinese gages (Hobart, 1985).

Optical Strain Measurement

Optical systems may not provide exact alternatives to resistance strain gages for all turbine engine applications, but they appear to have high potential for providing high temperature, noncontact, two-dimensional strain measuring systems with virtually unlimited strain range. An optical technique that requires no modification to the surface under test uses laser speckle patterns. These patterns are formed by constructive and destructive interference of laser light reflected from a diffuse surface. The source of the pattern is the irregularities in the surface; when the surface is distorted, for example by strain in the plane of the surface, the speckle pattern changes. Precise measurements of changes in recorded speckle patterns can provide information on the strain imposed on the surface. A practical implementation of this technique is a laser speckle photogrammetric system in which speckle patterns are recorded on photographic film (Stetson, 1983). Speckle pattern photographs (called specklegrams) are made at different increments of loading of the test sample and then pairs of specklegrams are examined in an automated interferometric photocomparator. The system uses heterodyne techniques to achieve accurate measurements to a fraction of an interference fringe. No attempt will be made here to describe this system in detail; it has been thoroughly described in the open literature (Stetson, 1983).

The laser speckle photogrammetric system has successfully measured high-temperature surface deformation. Stetson (1983) describes an experiment to measure the thermal expansion of an unrestrained plate of Hastelloy X at temperatures up to 1150 K. The plate was heated in a laboratory furnace to 1150 K and then allowed to cool to 500 K over a period of several hours. Specklegrams were recorded at roughly 200 K intervals during the heating and cooling and succeeding specklegram pairs were used to determine the thermal expansion of the plate. Measured thermal expanison agreed with values calculated from the measured temperature and the thermal expansion coefficient to within 3 percent.

We have attempted to use the laser speckle photogrammetric system in test cell environments. In one attempt we recorded specklegrams of a combustor liner in a high-temperature, high-pressure combustor test rig (Stetson, 1984). The specklegrams were taken through a viewing port in the pressure vessel of the test rig as combustor pressure and temperature were varied. A potential problem in this application is that the high-pressure cooling air flowing over the exterior surface of the combustor liner is in the optical viewing path, and turbulence in the gas flow may cause sufficient optical distortion to prevent correlation of succeeding pairs of specklegrams. Examples of undistorted and distorted specklegrams are shown in Figs. 18(a) and (b). This effect proved to be a fundamental limitation for the measuring system in this application when combustor pressure was higher than approximately 3 atm. We intend to explore further high temperature applications of optical strain measuring systems.

THIN FILM SENSORS

One of the fundamental precepts of experimentation is that the sensors used to get experimental data must not perturb the subject of the experiment from its condition prior to the introduction of the sensors. In turbine engine testing there are many situations in which this precept may be violated. A prime example is the measurement of turbine airfoil surface temperature. Conventional technology involves laying sheathed thermocouple wire into grooves cut into the surface of the airfoil, then covering the installation and smoothing the airfoil contour. Although the airfoil contour is restored, the thermocouple disturbs the temperature distribution, does not give a true measure of the outside surface temperature, and threatens the integrity of the structure of thin walled blades and vanes.

The thin film thermocouple shown in Fig. 19 appears to be an ideal solution for blade and vane surface temperature measurement (Grant and Przybyszewski, 1980; Grant et al., 1981; Grant et al., 1982). As seen in the cross-sectional sketch of the sensor in Fig. 20, the sensor has minimal intrusiveness. In this case the blade or vane, coated with an MCrAlY anticorrosion coating, is polished and then oxidized to form an adherent surface coating of aluminum oxide. Additional aluminum oxide is deposited over this film to form an electrically insulating film of roughly 2 μm thickness. Films of thermocouple alloy (Pt and Pt10%Rh) are sputter deposited through appropriate masks so that the films overlap at one point to form the thermocouple junction. The thermocouple films extend to the root of the vane where connections to conventional leadwires are made. Film-to-leadwire connections are made by parallel-gap welding. The complete installation of insulating film and thermocouple alloy films has a thickness of less than 20 μm. The installation has not changed the contour or the strength of the component and the greatest thermal changes apparent are the different absorptance and emittance of the thermocouple films compared to the oxidized MCrAlY surface. The technology for thin film thermocouples and turbine airfoils has been developed to the extent that instrumented vanes and blades are being used in turbine engine tests at temperatures up to 1250 K.

Thin film sensor development work is going on both at contractor facilities and at NASA Lewis. Figure 21 shows the thin film sensor laboratory at NASA Lewis. The laboratory is housed in a clean room in which both temperature and humidity are controlled. On the left in the photograph are three vacuum sputtering machines for deposition of both insulator and sensor films. In the right-hand corner of the room is equipment for photolithography of sensors; conventional photo-resist

techniques are used. At the far right edge of the photograph is a welder for connecting leadwires to sensor films.

CONCLUDING REMARKS

This paper has reviewed the state of development of a number of advanced instrumentation projects applicable to the hot sections of turbine engines. Most of these projects are complete and the instrumentation is in use. This is the case for the Combustor Viewing System, the Dynamic Gas Temperature Measuring System, total heat flux sensors, the laser anemometry projects described here, and thin film thermocouples. Work in the general area of thin film sensors is continuing in order to further improve the technology and expand sensor types and applications. The work to improve our high-temperature strain measuring capability is still in progress.

REFERENCES

Atkinson, W.H., and Strange, R.R., 1982, "Development of Advanced High-Temperature Heat Flux Sensors," NASA CR-165618.

Atkinson, W.H., Hobart, H.F., and Strange, R.R., 1983, "Advanced High Temperature Heat Flux Sensors," Proceedings of the 38th Instrument Society of America Conference, Advances in Instrumentation, Vol. 38, Part 2, Instrument Society of America, pp. 1457-1479.

Atkinson, W.H., Cyr, M.A., and Strange, R.R., 1984, "Turbine Blade and Vane Heat Flux Sensor Development, Phase I," NASA CR-168297.

Atkinson, W.H., Cyr, M.A., and Strange, R.R., 1985a, "Development of High-Temperature Heat Flux Sensors, Phase II - Verification Testing," NASA CR-174973.

Atkinson, W.H., Cyr, M.A., and Strange, R.R., 1985b, "Turbine Blade and Vane Heat Flux Sensor Development, Phase II," NASA CR-174995.

Elmore, D.L., Robinson, W.W., and Watkins, W.B., 1983, "Dynamic Gas Temperature Measurement System Final Report, Volume I Technical Efforts," NASA CR-168267.

Elmore, D.L., Robinson, W.W., and Watkins, W.B., 1984, "Dynamic Gas Temperature Measurement System," Proceedings of the 30th International Instrumentation Symposium, Instrumentation in the Aerospace Industry, Vol. 30, Advances in Test Measurements, Vol. 21, Instrument Society of America, pp. 289-302.

Elmore, D.L., Robinson, W.W., and Watkins, W.B., 1986a, "Further Development of the Dynamic Gas Temperature Measurement System, Vol. I Technical Efforts," NASA CR-179513.

Elmore, D.L., Robinson, W.W., and Watkins, W.B., 1986b, "Further Development of the Dynamic Gas Temperature Measurement System," AIAA Paper 86-1648.

Grant, H.P., and Przybyszewski, J.S., 1980, "Thin Film Temperature Sensor," NASA CR-159782.

Grant, H.P., Przybyszewski, J.S., and Claing, R.G., 1981, "Turbine Blade Temperature Measurements Using Thin Film Temperature Sensors," NASA CR-165201.

Grant, H.P., Przybyszewski, J.S., Claing, R.G., and Anderson, W.L., 1982, "Thin Film Temperature Sensors, Phase III," NASA CR-165476.

Hobart, H.F., 1985, "Evaluation Results of the 700°C Chinese Strain Gages," NASA TM-86973.

Holanda, R., 1984, "Analysis of Thermoelectric Properties of High-Temperature Complex Alloys of Nickel-Base, Iron-Base, and Cobalt-Base Groups," NASA TP-2278.

Hulse, C.O., Bailey, R.S., and Lemkey, F.D., 1985, "High Temperature Static Strain Gage Alloy Development Program," NASA CR-174833.

Hulse, C.O., et al., 1986, "Advanced High Temperature Static Strain Sensor Development," NASA CR-179520.

Hulse, C.O., Bailey, R.S., Grant, H.P., and Przybyszewski, J.S., 1987, "High Temperature Static Strain Gage Development Contract," NASA CR-180811.

Lading, L., 1983, "Estimating Time and Time-Lag in Time-of-Flight Velocimetry," Applied Optics, Vol. 22, No. 22, pp. 3637-3643.

Morey, W.W., 1984, "Hot Section Viewing System," NASA CR-174773.

Morey, W.W., 1985, "Jet Engine Combustor Viewing System," Conference on Lasers and Electro-Optics, IEEE, New York, p. 298.

Oberle, L.G., and Seasholtz, R.G., 1985, "Filter Induced Errors in Laser Anemometry Using Counter-Processor," International Symposium on Laser Anemometry, ASME FED Vol. 33, A. Dybbs and P.A. Pfund, eds., ASME, New York, pp. 221-230.

Oberle, L.G., 1987, "A Computer Controlled Signal Preprocessor for Laser Fringe Anemometer Applications," NASA TM-88982.

Seasholtz, R.G., Oberle, L.G., and Weikle, D.H., 1984, "Optimization of Fringe-Type Laser Anemometers for Turbine Engine Component Testing," AIAA Paper 84-1459. (NASA TM-83658).

Stetson, K.A., 1983, "The Use of Heterodyne Speckle Photogrammetry to Measure High-Temperature Strain Distributions," Holographic Data Nondestrutive Testing, D. Vukicevic, ed., Proc. SPIE-370, SPIE, Bellingham, WA, pp. 46-55.

Stetson, K.A., 1984, "Demonstration Test of Burner Liner Strain Measuring System," NASA CR-174743.

Stocks, D.R., and Elmore, D.L., 1986, "Further Development of the Dynamic Gas Temperature Measurement System, Vol. II - Computer Program User's Manual," NASA CR-179513-VOL-2.

Wernet, M.P., and Edwards, R.V., 1986, "Implementation of a New Type of Time-of-Flight Laser Anemometer," Applied Optics, Vol. 25, No. 5, pp. 644-648.

Wernet, M.P., 1987a, "Four Spot Laser Anemometer and Optical Access Techniques for Turbine Engine Applications," ICIASF '87, International Congress on Instrumentation in Aerospace Simulation Facilities, IEEE, New York, pp. 245-254. (NASA TM-88972).

Wernet, M.P., and Oberle, L.G., 1987b, "Laser Anemometry Techniques for Turbine Applications," ASME Paper 87-GT-241. (NASA TM-88953).

Wernet, M.P., and Seasholtz, R.G., 1987c, "Zoom Lens Compensator for a Cylindrical Window in Laser Anemometer Uses," Applied Optics, Vol. 26, No. 21, pp. 4603-4611.

Wu, T.T., Ma, L.C., and Zhao, L.B., 1981, "Development of Temperature Compensated Resistance Strain Gages for Use to 700°C," Experimental Mechanics, Vol. 21, No. 3, pp. 117-123.

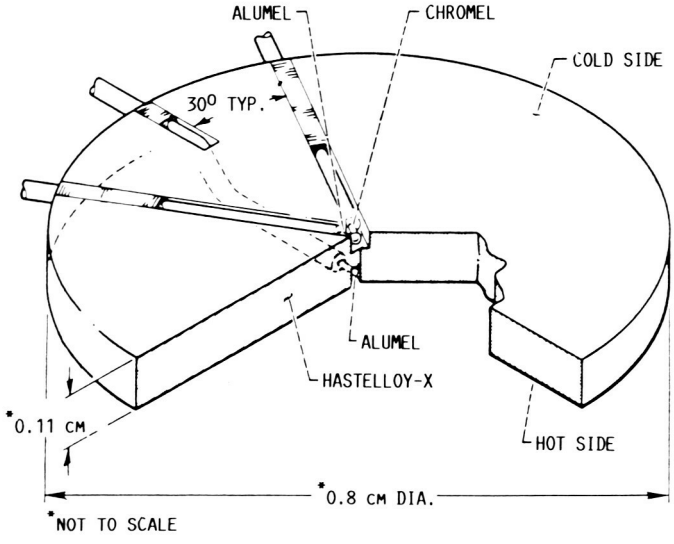

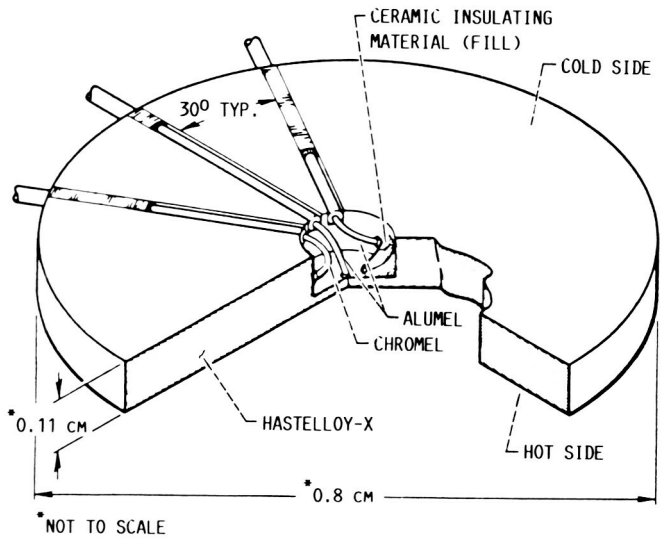

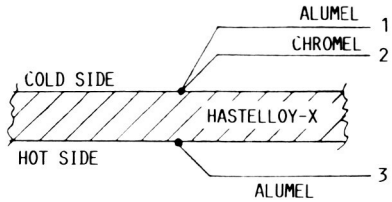

1-2 = $T_{REFERENCE}$
1-3 = SENSOR OUTPUT

FIGURE 1. - EMBEDDED THERMOCOUPLE HEAT FLUX SENSOR.

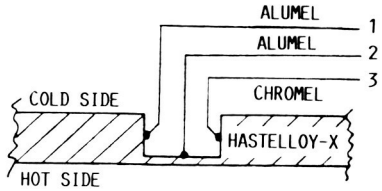

1-2 = SENSOR OUTPUT
1-3 = $T_{REFERENCE}$

FIGURE 2. - GARDON GAGE HEAT FLUX SENSOR.

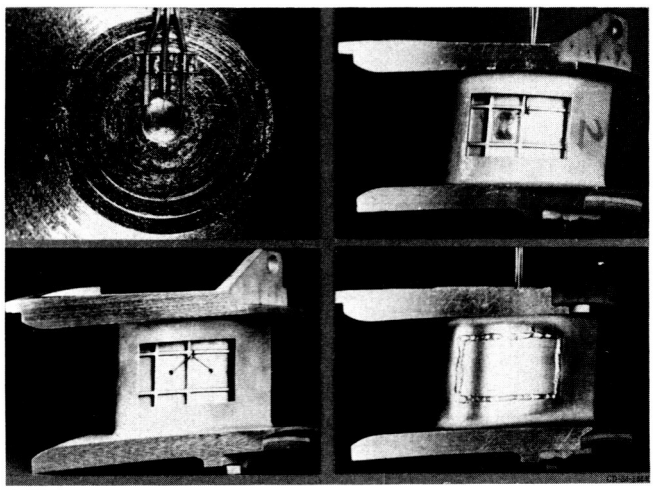

FIGURE 3. - HEAT FLUX SENSORS INSTALLED IN TURBINE VANE.

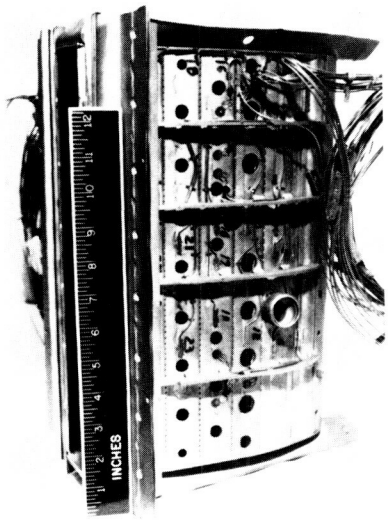

FIGURE 4. - COMBUSTOR SEGMENT INSTRUMENTED WITH HEAT FLUX SENSORS.

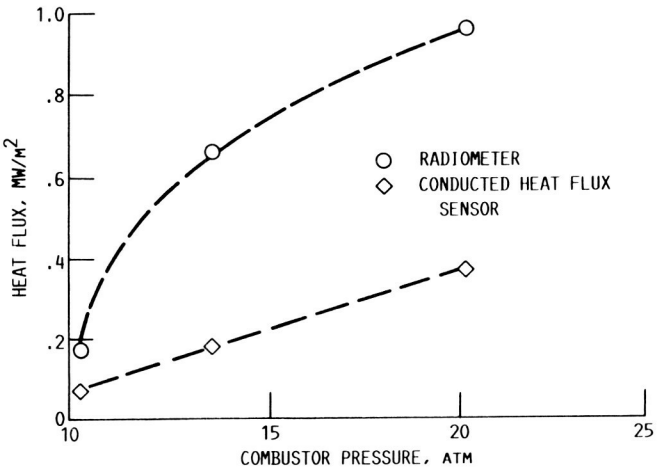

FIGURE 5. - COMPARISON OF HEAT FLUX CONDUCTED THROUGH THE COMBUSTOR LINER AND INCIDENT RADIANT HEAT FLUX FOR VARIOUS LEVELS OF COMBUSTOR PRESSURE. RADIANT HEAT FLUX WAS MEASURED WITH A COMMERCIAL RADIOMETER.

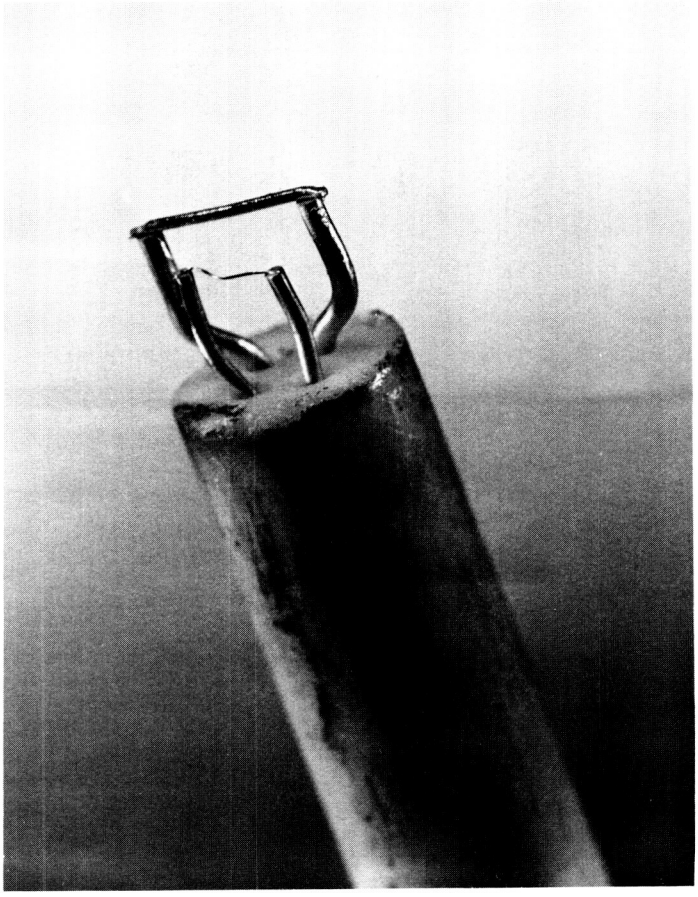

FIGURE 6. - DUAL ELEMENT THERMOCOUPLE PROBE FOR MEASURING FLUCTUATING GAS TEMPERATURE.

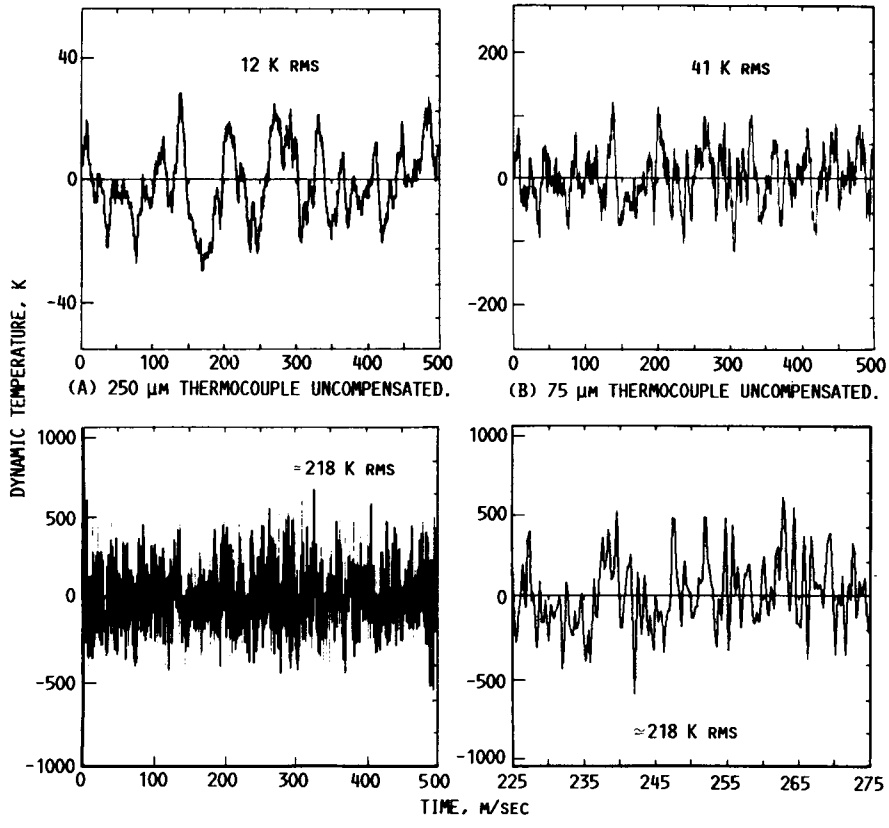

FIGURE 7. - DYNAMIC GAS TEMPERATURE SIGNALS FROM AN ENGINE TEST.

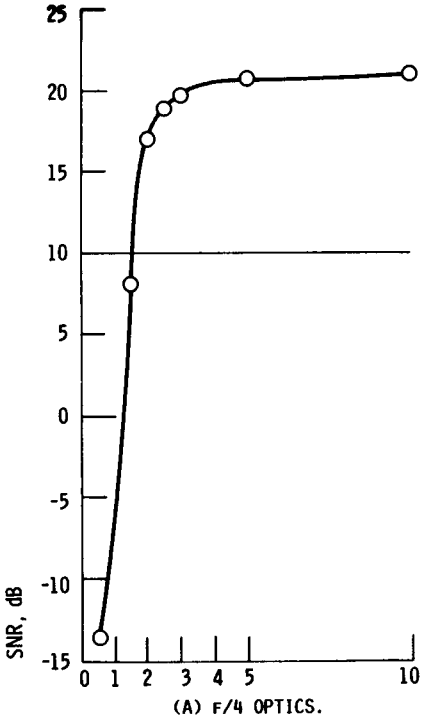

FIGURE 8. - SIGNAL-TO-NOISE RATIO (SNR) FOR OPTIMUM MASK VERSUS DISTANCE OF PROBE VOLUME FROM WALL.

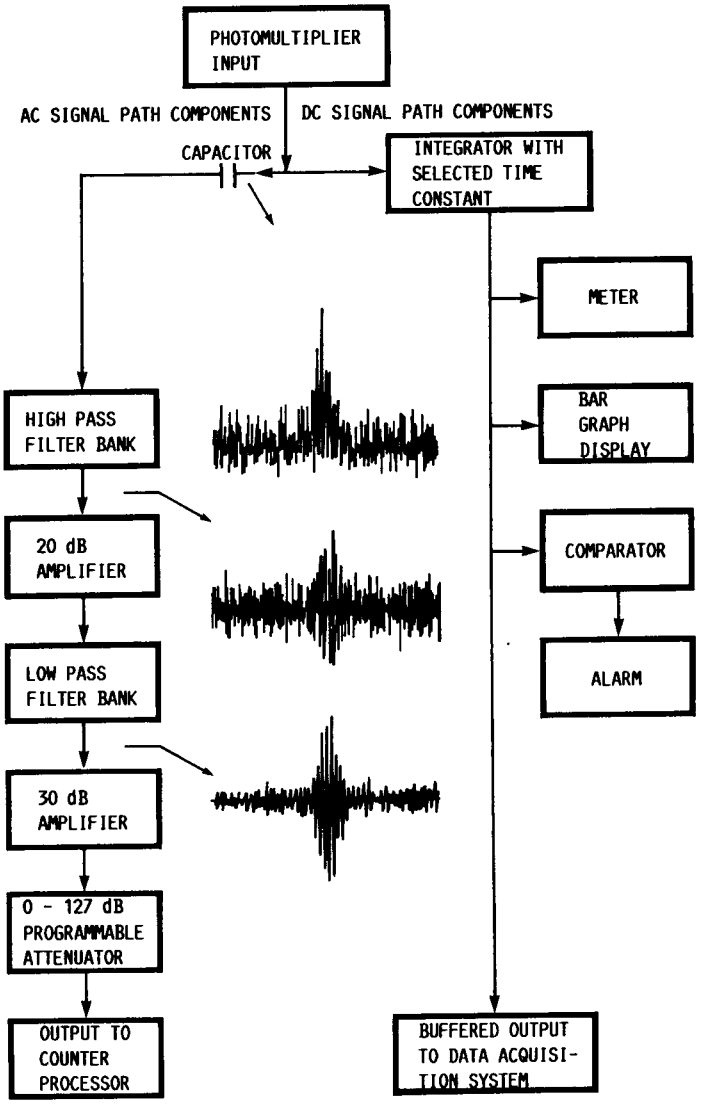

FIGURE 9. - LASER FRINGE ANEMOMETER PRE-PROCESSOR SIGNAL FLOW DIAGRAM SHOWING THE DOPPLER SIGNAL IN THE TIME DOMAIN AT THREE POINTS IN THE SIGNAL FLOW.

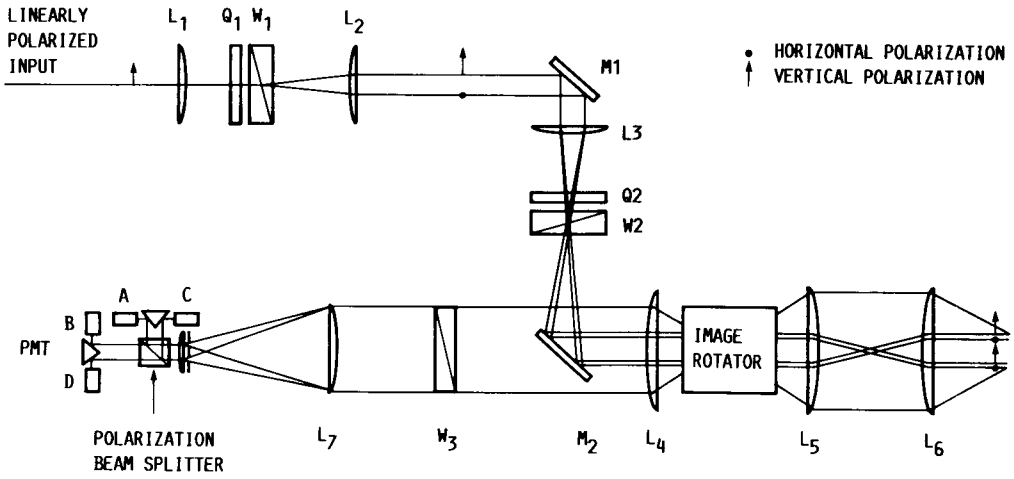

FIGURE 10. - SCHEMATIC VIEW OF THE TRANSMITTING AND RECEIVING OPTICS.

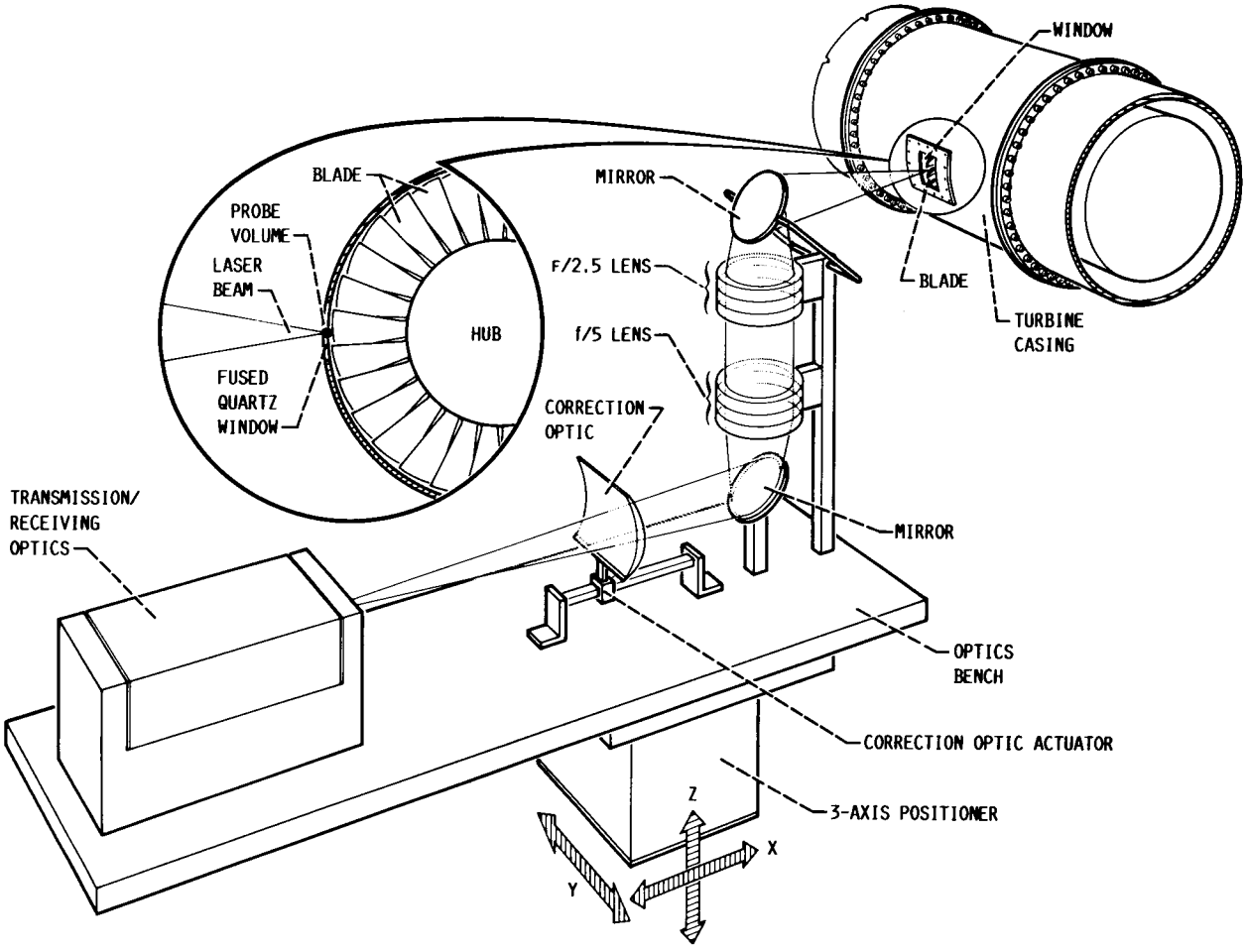

FIGURE 11. - SCHEMATIC VIEW OF A LASER ANEMOMETER SYSTEM APPLIED TO A TURBINE RIG INCORPORATING A CURVE CASING WINDOW. THE ABERRATIONS INDUCED BY THE TURBINE WINDOW ARE COMPENSATED FOR BY THE CORRECTION OPTIC. AS THE 3-AXIS TABLE SCANS THE PROBE VOLUME THROUGH THE BLADE PASSAGE, THE CORRECTION OPTIC POSITION IS ADJUSTED BY ANOTHER ACTUATOR. IN THIS POSITION, THE PROBE VOLUME IS JUST INSIDE THE TURBINE WINDOW, AND THE ACTUATOR IS AT ITS FURTHEST POSITION FROM THE F/5 LENS.

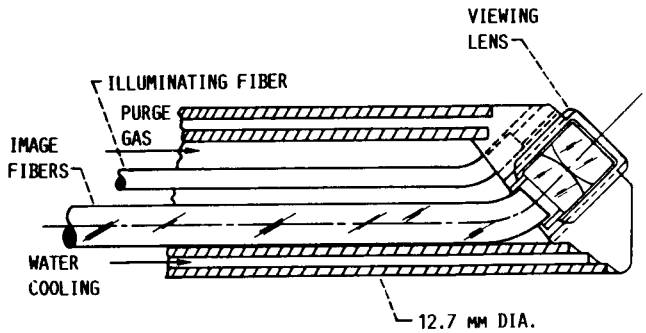

FIGURE 12(A). - CROSS SECTION OF WIDE FIELD OF VIEW COMBUSTOR VIEWING PROBE.

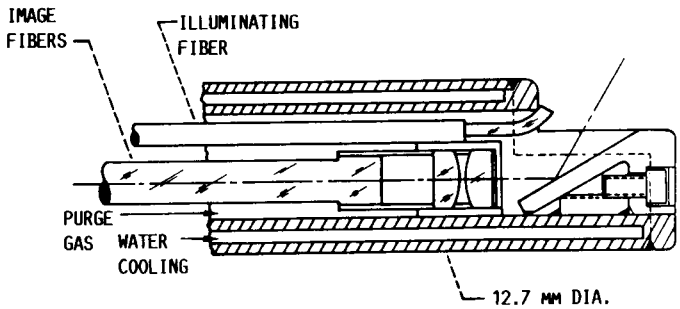

FIGURE 12(B). - CROSS SECTION OF NARROW FIELD OF VIEW COMBUSTOR VIEWING PROBE.

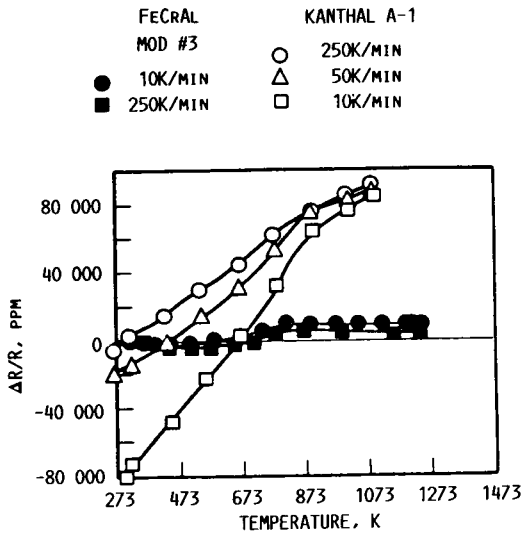

FIGURE 13. - FRACTIONAL RESISTANCE CHANGE OF KANTHAL A-1 AND FECRAL MOD #3 AS A FUNCTION OF TEMPERATURE.

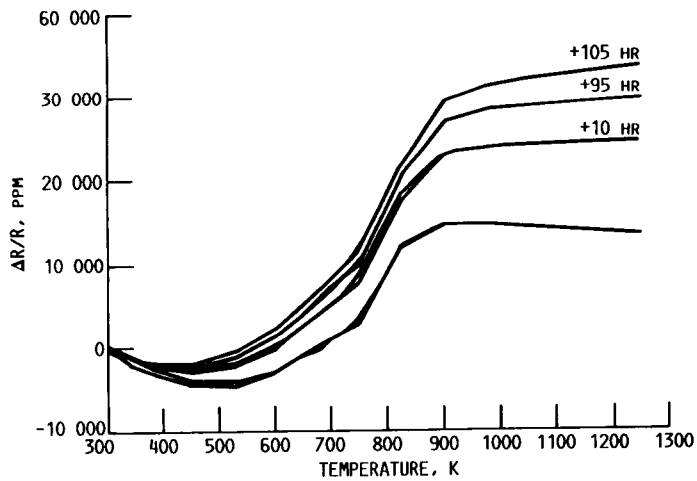

FIGURE 14. - EFFECT OF SOAK TIME AT 1250 K ON THE RESISTANCE VERSUS TEMPERATURE CHARACTERISTIC OF FECRAL MOD #3.

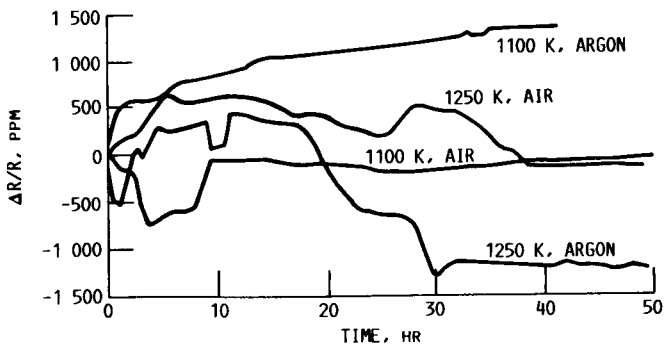

FIGURE 15. - LONG-TERM RESISTANCE DRIFT OF PDCR ALLOY IN ARGON AND AIR.

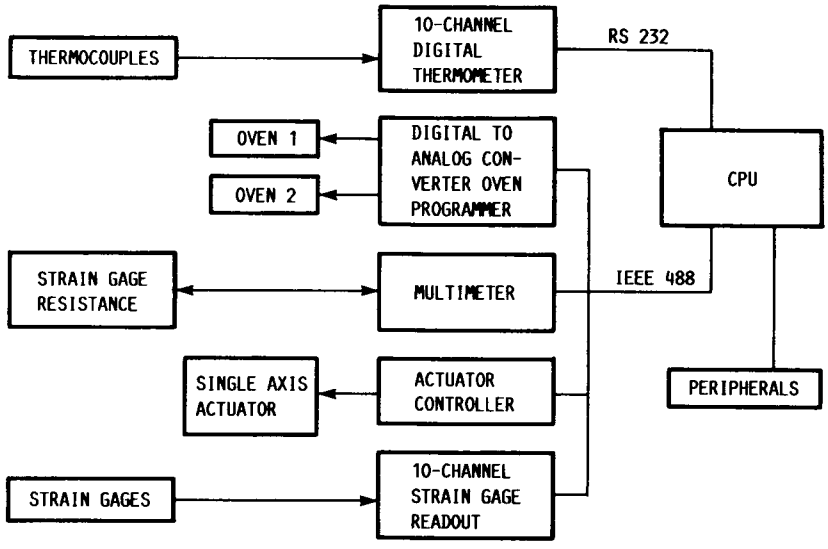

FIGURE 16. - BLOCK DIAGRAM OF THE HIGH TEMPERATURE STRAIN GAGE TESTING SYSTEM.

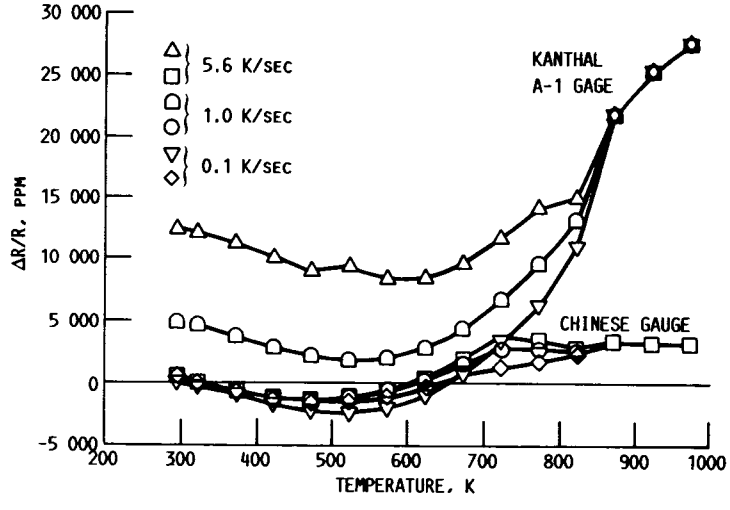

FIGURE 17. - FRACTIONAL RESISTANCE CHANGE VERSUS TEMPERATURE FOR KANTHAL A-1 AND 700 ^{o}C CHINESE GAGES WITH THREE DIFFERENT COOLING RATES.

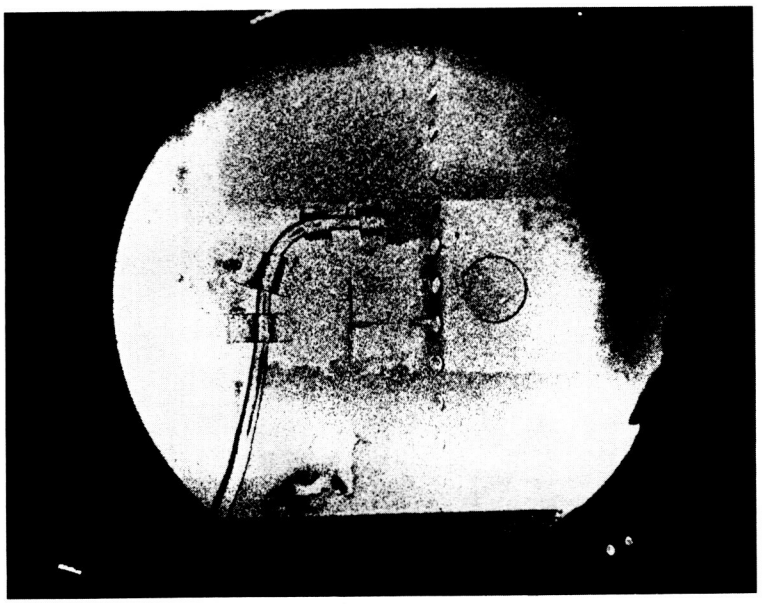

FIGURE 18(A). - SPECKLEGRAM OF COMBUSTOR LINER WITH NO DISTORTION DUE TO FLOW.

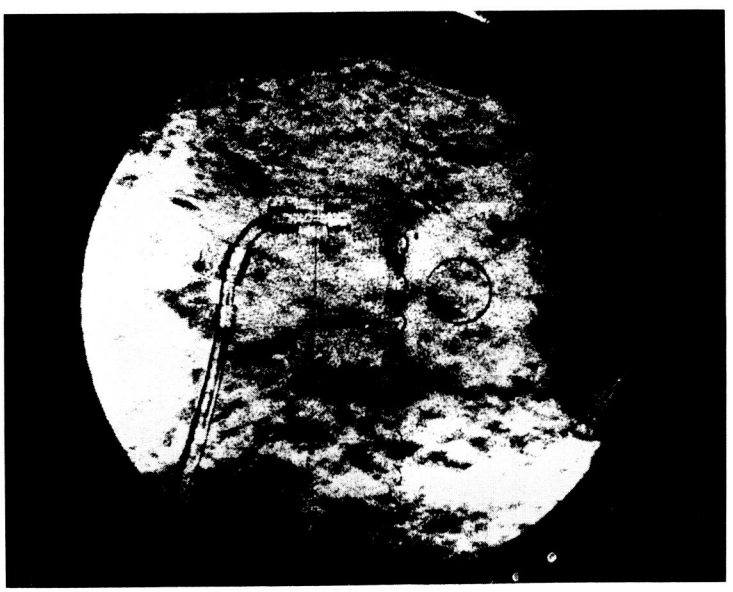

FIGURE 18(B). - SPECKLEGRAM OF COMBUSTOR LINER WITH DISTORTION FROM TURBULENT GAS FLOW.

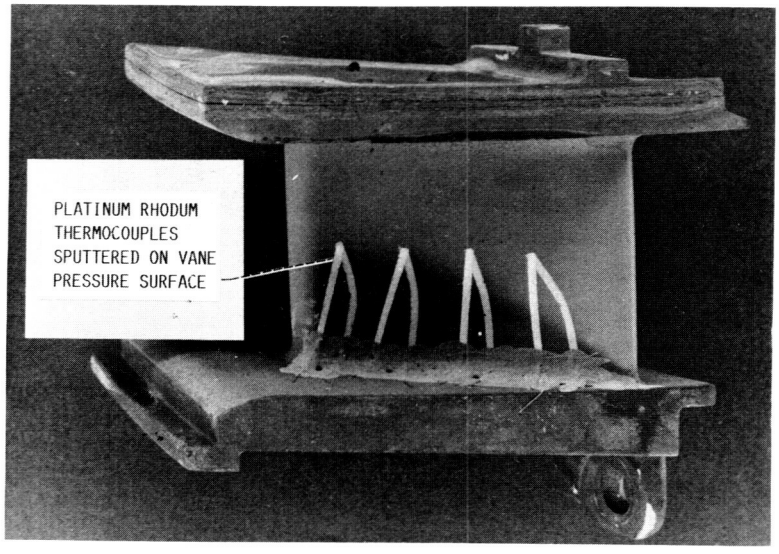

FIGURE 19. - A TURBINE VANE INSTRUMENTED WITH THIN FILM THERMOCOUPLES.

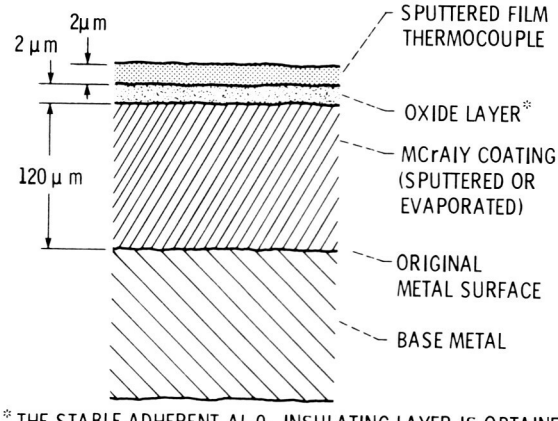

* THE STABLE ADHERENT Al_2O_3 INSULATING LAYER IS OBTAINED BY AT LEAST 50-hr OXIDATION (AT 1300 K) OF THE COATING. FOLLOWED BY Al_2O_3 SPUTTERING.

FIGURE 20. - THIN FILM THERMOCOUPLE CROSS SECTION.

FIGURE 21. - THIN FILM SENSOR LABORATORY AT THE LEWIS RESEARCH CENTER.